Measurement and Characterization of Laser Chirp of Multiquantum-Well Distributed-Feedback Lasers

Eva Peral and Amnon Yariv, *Fellow, IEEE*

***Abstract*—Measurements of relative intensity noise and modulation response, before and after propagation in optical fiber, of the output field of multiquantum-well distributed-feedback (MQW-DFB) lasers are used to determine the influence of the intraband damping mechanisms, the DFB structure and the carrier transport and carrier capture into the QW's on the laser chirp. The power dependence of the linewidth enhancement factor is shown to explain the saturation of the laser linewidth at high optical powers.**

***Index Terms*—Laser measurements, optical fiber measurement applications, optical fiber communication, optical modulation, distributed-feedback lasers, quantum-well lasers, semiconductor lasers.**

I. Introduction

RECENT investigation of multiquantum-well distributed-feedback (MQW-DFB) lasers suggests that the laser dynamics are affected by intraband damping mechanisms such as spectral hole burning and carrier heating, longitudinal spatial variations of the optical intensity and/or carrier density due to the DFB structure, and carrier transport and quantum carrier capture into the quantum wells (QW's).

The chirp to intensity modulation index ratio (CIR) determines the small-signal modulation response (MR) of directly modulated lasers and the relative intensity noise (RIN) after propagation through an optical filter [1]. Although some analytical expressions have been proposed to model the CIR of DFB lasers, in practice it is necessary to perform numerical simulations to determine the laser chirp precisely. On the other hand, a simplified model has been proposed that accurately explains the carrier dynamics of MQW lasers and results in analytical expressions for the intensity modulation (IM) [2] and frequency modulation (FM) [3] of the laser.

In this letter, we derive expressions for the CIR of MQW lasers and give experimental evidence of the importance of the effect of the capture time into the QW's on RIN and MR after fiber and laser linewidth compared to intraband damping mechanisms and spatial hole burning. Inclusion of all these effects allows precise determination of the linewidth enhancement factor, α_N, from measurements of RIN and MR after fiber. The power dependence of α_N is shown to explain the increase of linewidth at high optical powers.

Manuscript received October 8, 1998; revised November 23, 1998. This work was based on work that was supported by the Advanced Research Projects Agency, by the Office of Naval Research, and by the Air Force Office of Scientific Research under Award N00014-91-J-1195. The work of R. Leheny was supported by the Defense Advanced Research Projects Agency, the work of Y. S. Park was supported by the Office of Naval Research, and the work of H. Schlossberg was supported by the Air Force Office of Scientific Research.

The authors are with the Department of Applied Physics, California Institute of Technology, Pasadena, CA 91125 USA.

Publisher Item Identifier S 1041-1135(99)01864-9.

II. Theory

In [2], effective small-signal rate equations for a directly modulated single-quantum-well laser were derived. Following the same approach, and neglecting diffusion along the barriers and the effect of the DFB structure, it can be shown that the same equations apply to MQW lasers with

$$\tau_{\rm cap} = \eta_V \tau_{\rm cap}^Q + \frac{L_{\rm SCH}^2}{8D}$$

and

$$R_{\rm ce} = \frac{\tau_{\rm cap}}{\tau_{\rm esc}} = \eta_V \frac{\tau_{\rm cap}^Q}{\tau_{\rm esc}^Q}.$$

Here, $\tau_{\rm cap}^Q$ and $\tau_{\rm esc}^Q$ are the intrinsic quantum capture and escape times, $\tau_{\rm cap}$ and $\tau_{\rm esc}$ are the effective capture and escape times, $\eta_V = V_{\rm SCH}/V_{\rm QW}$ is the ratio between the volume of the separate-confinement heterostructure (SCH) region and the total volume of the quantum wells, $L_{\rm SCH}$ is the length of the SCH region and D is the diffusion coefficient.

From the effective small-signal rate equations at modulation angular frequency Ω, the photon density variation, ΔP, and the carrier density variation in wells, ΔN_w, and barriers, ΔN_b, can be derived and are given by

$$\Delta P = \frac{\Gamma_w G_N P \frac{\Delta I_Q(\Omega)}{eV_{\rm QW}} + \frac{\Gamma_w F_P}{V_{\rm QW}}\left(i\Omega + \frac{1}{\tau_{\rm nw}} + \frac{1}{\tau_Q(\Omega)}\right)}{D_0 + \frac{1}{\tau_Q(\Omega)}(i\Omega + \Gamma_w G_P P)} \quad (1)$$

$$\Delta N_w = \frac{1}{\Gamma_w G_N P}\left[(i\Omega + \Gamma_w G_P P)\Delta P - \frac{\Gamma_w F_P}{V_{\rm QW}}\right] \quad (2)$$

$$\eta_V \Delta N_b = \frac{R_{\rm ce}}{1 + \tau_{\rm cap}/\tau_{\rm nb} + i\Omega\tau_{\rm cap}}\Delta N_w + \tau_{\rm cap}\frac{\Delta I_Q(\Omega)}{eV_{\rm QW}} \quad (3)$$

where the effective current injection into the QW's is $\Delta I_Q(\Omega) = \Delta I/(1 + \tau_{\rm cap}/\tau_{\rm nb} + i\Omega\tau_{\rm cap})$ and the effective nonradiative recombination rate due to the finite capture time in the QW's is

$$\frac{1}{\tau_Q(\Omega)} = R_{\rm ce}\frac{i\Omega + 1/\tau_{\rm nb}}{1 + \tau_{\rm cap}/\tau_{\rm nb} + i\Omega\tau_{\rm cap}}.$$

Here, ΔI is the modulation current; F_P is a Langevin photon noise source; $D_0 = (i\Omega)^2 + i\Omega\gamma_0 + \Omega_0^2$ is the resonant denominator of the modulation response when quantum capture effects are neglected, with

$$\Omega_0^2 = \frac{G_N P}{\tau_{\rm ph}} + \frac{\Gamma_w G_P P}{\tau_{\rm nw}}$$

the relaxation frequency squared, and

$$\gamma_0 = \frac{1}{\tau_{\rm nw}} + \Gamma_w G_P P + G_N P$$

the damping coefficient; P is the average photon density; $G_N = \partial G/\partial N_w$ is the differential gain with G the stimulated recombination rate in the well; $G_P = -\partial G/\partial P$ describes the dependence of G on photon density; Γ_w is the confinement factor of the carriers in the QW's and $\tau_{\rm nw}$ and $\tau_{\rm nb}$ are the differential carrier lifetimes in wells and barriers, respectively.

Frequency variations, $\Delta\omega$, are affected by changes in carrier density, ΔN_w and ΔN_b, and photon density, ΔP, and thus obey

$$\Delta\omega = -\frac{\omega}{n_g}\Delta n' = -\frac{\omega}{n_g}\left[\Gamma_w \frac{\partial n'}{\partial N_w}\Delta N_w + \Gamma_{\rm sch}\frac{\partial n'}{\partial N_b}\Delta N_b + \Gamma_w \frac{\partial n'}{\partial P}\Delta P\right] + F_\phi \quad (4)$$

where n_g is the group index, n' is the real part of the effective modal refractive index, ω is the optical frequency, $\Gamma_{\rm sch}$ is the confinement factor of the carriers in the SCH region and F_ϕ is a Langevin noise source for frequency fluctuations. In (4), the last factor in the term in brackets accounts for the power dependence of the gain in the QW's, which through a Kramers–Kronig transformation results in a change in n'.

Propagation in dispersive fiber results in conversion of part of the FM into IM. The detected photocurrent at modulation frequency Ω, $\Delta I_{\rm ph}$, after propagation, is related to fiber parameters and also to the chirp to intensity modulation index ratio ${\rm CIR} = \Delta\omega/(\Delta P/P)$ as follows [1]:

$$\frac{\Delta I_{\rm ph}(\Omega, z)}{\Delta I_{\rm ph}(\Omega, 0)} = \cos\theta - 2\frac{1}{i\Omega}\frac{\Delta\omega}{\Delta P/P}\sin\theta \quad (5)$$

where $\theta(\Omega, z) = -\frac{1}{2}\beta_2\Omega^2 z$, β_2 is the group velocity dispersion parameter and z is the fiber length. In the following we will derive the CIR due current and photon variations for MQW lasers, which determine the small-signal MR and RIN after fiber (or any other filter, as explained in [1], [4]), respectively.

Substituting (1)–(3) into (4), we find that the CIR due to current variations, ΔI, is given by

$${\rm CIR}|_{\Delta I} = \left.\frac{\Delta\omega}{\Delta P/P}\right|_{\Delta I} = -\frac{\alpha_N}{2}[(i\Omega + \Gamma_w G_P P)(1 + R_{\rm ce}\xi) + \xi\tau_{\rm cap}D_0] + \frac{\alpha_P}{2}\Gamma_w G_P P \quad (6)$$

where

$$\alpha_N = \frac{\partial n'}{\partial N_w}\Big/\frac{\partial n''}{\partial N_w}$$

is the linewidth enhancement factor with n'' the imaginary part of the effective refractive index,

$$\alpha_P = \frac{\partial n'}{\partial P}\Big/\frac{\partial n''}{\partial P}$$

and ξ is related to the ratio between the refractive index change due to a change in carriers in barrier and in well as

$$\xi = \frac{1}{\eta_V}\frac{\Gamma_{\rm sch}}{\Gamma_w}\frac{\partial n'}{\partial N_b}\Big/\frac{\partial n'}{\partial N_w} \cong \frac{\partial n'}{\partial N_b}\Big/\frac{\partial n'}{\partial N_w}. \quad (7)$$

The CIR due to photon fluctuations is given by

$${\rm CIR}|_{F_P} = \left.\frac{\Delta\omega}{\Delta P/P}\right|_{F_P} = \frac{\alpha_N}{2}G_N P\frac{i\Omega + 1/\tau_{\rm ph}}{i\Omega + 1/\tau_Q} \times\left[1 + \frac{R_{\rm ce}\xi}{1 + i\Omega\tau_{\rm cap} + \tau_{\rm cap}/\tau_{\rm nb}}\right]. \quad (8)$$

where $\tau_{\rm ph} = 1/\Gamma_w G$ is the photon lifetime.

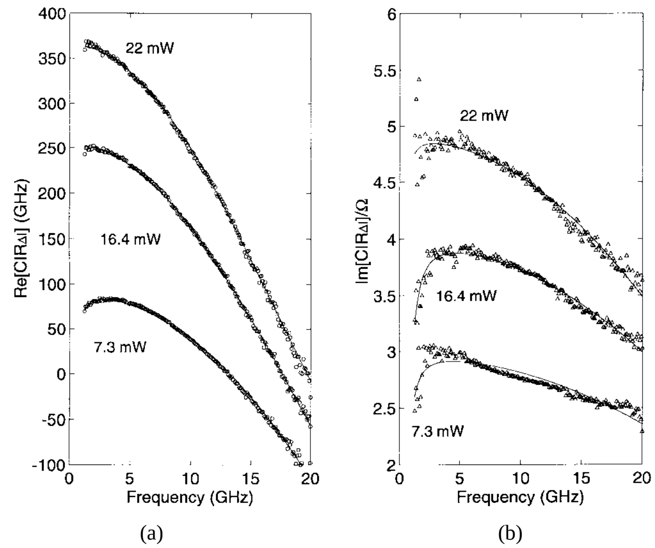

Fig. 1. (a) Real part of ${\rm CIR}|_{\Delta I}$ and (b) imaginary part of ${\rm CIR}|_{\Delta I}$ divided by Ω as a function of modulation frequency for several optical powers (measured at laser output facet). Solid line is the fitting.

Finally, the laser linewidth is also affected by the changes in carrier density in the barrier as follows:

$$\Delta\nu = \Delta\nu_{\rm ST}\left[1 + (1 + R_{\rm ce}\xi)^2\alpha_N^2\right] = \Delta\nu_{\rm ST}\left[1 + \alpha_{N{\rm eff}}^2\right] \quad (9)$$

where $\Delta\nu_{\rm ST}$ is the Shallow–Townes linewidth.

Equation (3) indicates that the carrier density in the barrier, ΔN_b, is comprised of two terms. The first one follows the dynamics of the carrier density in the well and results in an increase in the effective linewidth enhancement factor obtained from measurement of the linewidth by a factor $\alpha_{N{\rm eff}}/\alpha_N = 1 + R_{\rm ce}\xi$, as observed in (9). For small capture times, this is also the effect on RIN. The second term of ΔN_b in (3) follows the current modulation signal and has an important effect on the MR after fiber, which is reflected in the term proportional to the resonant denominator of the MR, D_0, in (6).

III. Experiment

Several 250-μm-long single-mode MQW-DFB lasers at 1.55 μm with high-reflection and antireflection coatings on the facets were used in the experiments. The ${\rm CIR}|_{\Delta I}$ was measured as explained in [1] and is shown in Fig. 1 for several laser output powers. According to (6), the ${\rm CIR}|_{\Delta I}$ is described by a second-order polynomial in $i\Omega$. However, it was found that the experimental data is more precisely described by a higher order polynomial such as ${\rm CIR}|_{\Delta I} = c_{-2}(i\Omega)^{-2} + c_0 + c_1(i\Omega) + c_2(i\Omega)^2 + c_3(i\Omega)^3$. Numerical simulations including both the effects of the quantum capture time and the DFB structure for the lasers tested indicate that the additional coefficients can be attributed to the DFB structure. Nevertheless, it was found that, for our lasers, (6) can well approximate the ${\rm CIR}|_{\Delta I}$, and it was not necessary to include spatial hole burning. Thus, approximate expressions for c_0, c_1 and c_2 can be derived from (6).

Measurements of RIN at the laser output, which are parasitic-free as opposed to the MR, were used to determine Ω_0, γ_0, $\tau_{\rm nw}$, and $\Delta\nu_{\rm ST}$. The photon lifetime, $\tau_{\rm ph}$, and $R_{\rm ce}$ were determined so as to obtain best agreement among the

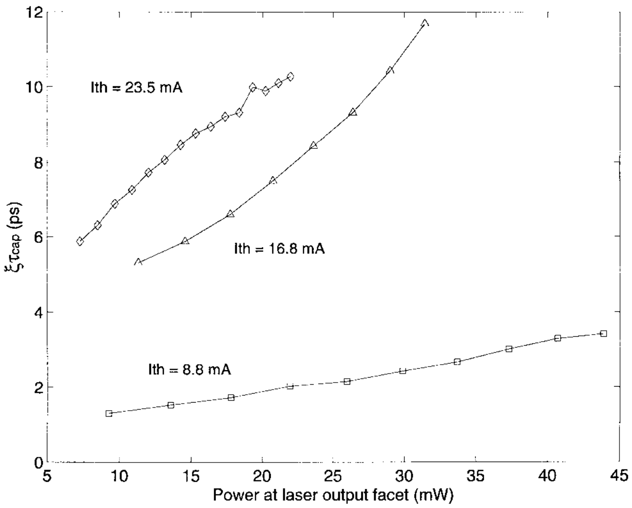

Fig. 2. Linewidth enhancement factor as determined from c_0 (circles), c_1 (squares), RIN after fiber (triangles) and linewidth (diamonds). The inset shows the measured linewidth, and the expected linewidth (solid) with power independent α_N.

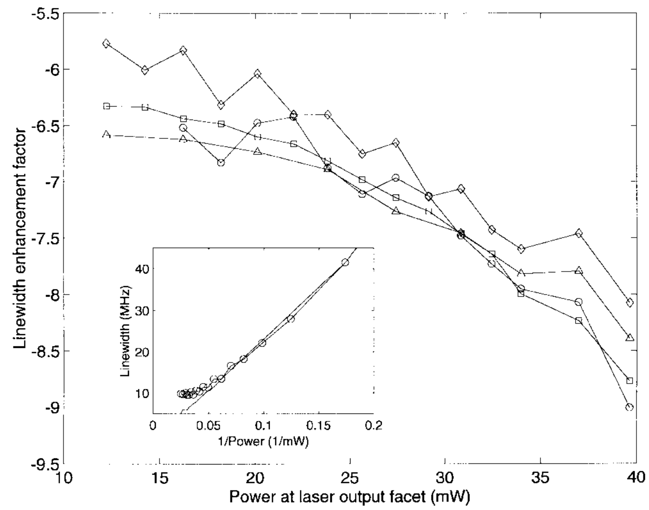

Fig. 3. Measured $\xi\tau_{\rm cap}$ for three MQW-DFB lasers with different threshold intensities.

value for $\alpha_{N\rm eff}$ obtained from the coefficients c_0 and c_1, and that obtained from measurement of RIN after propagation in dispersive fiber [4]. The values reported for $R_{\rm ce}$ in the literature vary from 0.01 to 0.5. For our lasers, we found that $R_{\rm ce}$ was negligibly small, and as a consequence, we can approximate $1/\tau_Q \approx 0$ in (1) and (8).

The linewidth was measured using a self-heterodyne technique. The Lorentzian part of the linewidth was determined by fitting the lineshape to a Voigt profile, and α_N was determined using (9). The values for α_N obtained from measurements of linewidth, c_0, c_1 and RIN after fiber are shown in Fig. 2 as a function of laser output power. Agreement of all the four measurements is found. The inset shows the measured linewidth, which saturates at high powers. The solid line is the linewidth that would be obtained if α_N had a constant value equal to that at low powers. Thus, the power dependence of α_N can explain the saturation of the linewidth at high optical powers. It was found that the power dependence of α_N originates mainly from the power dependence of G_N, as determined from Ω_0, which is also expected theoretically, since the carrier density in the wells is clamped and as a consequence $\partial n'/\partial N_w$ is practically independent of optical power.

The measured c_2 has a strong dependence on optical power that cannot be explained by the power dependence of α_N. Fig. 3 shows $\xi\tau_{\rm cap}$ for three different lasers. The value of $\xi\tau_{\rm cap}$ increases as the optical power increases, and seems to correlate with the laser threshold intensity, i.e., carrier density. As opposed to the carrier density in the wells N_w, the carrier density in the barriers N_b is not clamped, but increases with current injection I, as $\eta_V N_b \cong R_{\rm ce}N_w + \tau_{\rm cap}I/eV_{\rm sch}$. Above a critical carrier density, which for our lasers is estimated at $N_b \approx 5 \times 10^{16}$ cm^{-3}, bandgap shrinkage effects contribute to a strong increase of the magnitude of $\partial n'/\partial N_b$ with carrier density in the barrier [5]. On the other hand, $\tau_{\rm cap}$ is expected to increase for larger carrier density in the barrier due to a smaller diffusion coefficient and a larger quantum capture time [6]. We have corroborated that a combination of both effects can explain the power dependence of $\xi\tau_{\rm cap}$ in Fig. 3. However, both contributions are difficult to separate and an independent measurement of ξ or $\tau_{\rm cap}$ is needed to determine their dependence on optical power, which will be the subject of future research.

IV. Conclusion

The effect of the effective capture time into the quantum wells of MQW-DFB lasers on RIN and MR after propagation in dispersive fiber was studied theoretically and experimentally. The power dependence of the linewidth enhancement factor and effective capture time of MQW-DFB lasers was studied. The power dependence of the linewidth enhancement factor was able to explain the saturation of the linewidth at high powers.

Acknowledgment

The authors are grateful to Ortel Corporation, in particular to Dr. J. Ianelli and Dr. T. R. Chen, for providing the lasers. They also thank Dr. W. Marshall for many useful discussions.

References

[1] E. Peral, W. K. Marshall, and A. Yariv, "Precise measurement of semiconductor laser chirp using effect of propagation in dispersive fiber and application to simulation of transmission through fiber gratings," *J. Lightwave Technol.*, vol. 16, pp. 1874–1880, Oct. 1998.

[2] K. Lau, "Dynamics of quantum well lasers," in *Quantum Well Lasers*, P. S. Zory, Ed. San Diego, CA: Academic, 1993.

[3] R. F. S. Ribeiro, J. R. F. da Rocha, A. V. T. Cartaxo, H. J. A. da Silva, B. Franz, and B. Wedding, "FM response of quantum-well lasers taking into account carrier transport effects," *IEEE Photon. Technol. Lett.*, vol. 7, pp. 857–859, Aug. 1995.

[4] E. Peral, W. K. Marshall, D. Provenzano, and A. Yariv, "Effect of many weak side modes on relative intensity noise of distributed feedback semiconductor lasers," *Appl. Phys. Lett.*, vol. 72, no. 8, pp. 888–890, Feb. 1998.

[5] Bennett, Soref, and Alamo, "Carrier induced change in refractive index of InP, GaAs, and InAsAsP," *IEEE J. Quantum Electron.*, vol. 26, pp. 113–122, Jan. 1990.

[6] J. Wang, U. A. Griesinger, F. Stolz, and H. C. Shweizer, "Carrier capture times in quantum-well, -wire, and -box dstribute feedback lasers characterized by dynamic lasing emission measurements," *IEEE J. Select. Topics Quantum Electron.*, vol. 3, pp. 223–229, Apr. 1997.